Received: 10 December 2019 | Revised: 28 April 2020 | Accepted: 29 April 2020

DOI: 10.1096/fj.201903074RR

RESEARCH ARTICLE

THE FASEB JOURNAL

Systemic blockade of ACVR2B ligands attenuates muscle wasting in ischemic heart failure without compromising cardiac function

Zoltán Szabó[1] | Laura Vainio[1] | Ruizhu Lin[1,2] | Julia Swan[1,3] | Juha J. Hulmi[4,5] | Lea Rahtu-Korpela[1] | Raisa Serpi[3,6] | Mika Laitinen[7,8] | Arja Pasternack[5] | Olli Ritvos[5] | Risto Kerkelä[1,2] | Johanna Magga[1,3]

[1]Research Unit of Biomedicine, Department of Pharmacology and Toxicology, University of Oulu, Oulu, Finland

[2]Medical Research Center Oulu, Oulu University Hospital and University of Oulu, Oulu, Finland

[3]Biocenter Oulu, University of Oulu, Oulu, Finland

[4]Faculty of Sport and Health Sciences, Neuromuscular Research Center, University of Jyväskylä, Jyväskylä, Finland

[5]Department of Physiology, Faculty of Medicine, University of Helsinki, Helsinki, Finland

[6]Faculty of Biochemistry and Molecular Medicine, University of Oulu, Oulu, Finland

[7]Department of Medicine, University of Helsinki, Helsinki, Finland

[8]Department of Medicine, Helsinki University Hospital, Helsinki, Finland

Correspondence
Johanna Magga, Research Unit of Biomedicine, Department of Pharmacology and Toxicology, Aapistie 5B, P.O.Box 5000, 90220 Oulu, Finland.
Email: Johanna.Magga@oulu.fi

Funding information
Academy of Finland (Suomen Akatemia), Grant/Award Number: 268505, 297094 and 275922; Sydäntutkimussäätiö (Finnish Foundation for Cardiovascular Research)

Abstract

Signaling through activin receptors regulates skeletal muscle mass and activin receptor 2B (ACVR2B) ligands are also suggested to participate in myocardial infarction (MI) pathology in the heart. In this study, we determined the effect of systemic blockade of ACVR2B ligands on cardiac function in experimental MI, and defined its efficacy to revert muscle wasting in ischemic heart failure (HF). Mice were treated with soluble ACVR2B decoy receptor (ACVR2B-Fc) to study its effect on post-MI cardiac remodeling and on later HF. Cardiac function was determined with echocardiography, and myocardium analyzed with histological and biochemical methods for hypertrophy and fibrosis. Pharmacological blockade of ACVR2B ligands did not rescue the heart from ischemic injury or alleviate post-MI remodeling and ischemic HF. Collectively, ACVR2B-Fc did not affect cardiomyocyte hypertrophy, fibrosis, angiogenesis, nor factors associated with cardiac regeneration except modification of certain genes involved in metabolism or cell growth/survival. ACVR2B-Fc, however, was able to reduce skeletal muscle wasting in chronic ischemic HF, accompanied by reduced LC3II as a marker of autophagy and increased mTOR signaling and

Abbreviations: ACVR2B, activin receptor 2B; ACVR2B-Fc, activin receptor 2B decoy receptor; GDF, growth differentiation factor; GDF8, growth differentiation factor8; myostatin; HF, heart failure; Inhba, inhibin betaa; activin A; Inhbb, inhibin betab; activin B; IR, ischemia-reperfusion; LAD, left anterior descending coronary artery; MHC, myosin heavy chain; MI, myocardial infarction; mTOR, mammalian target of rapamycin; PGC1α, peroxisome proliferator-activated receptor gamma coactivator 1 alpha; TGFβ, transforming growth factor-β; WGA, wheat germ agglutinin.

Work was done at University of Oulu, Oulu, Finland.

Cited4 expression as markers of physiological hypertrophy in quadriceps muscle. Our results ascertain pharmacological blockade of ACVR2B ligands as a possible therapy for skeletal muscle wasting in ischemic HF. Pharmacological blockade of ACVR2B ligands preserved myofiber size in ischemic HF, but did not compromise cardiac function nor exacerbate cardiac remodeling after ischemic injury.

KEYWORDS

activins, growth differentiation factors, myocardial infarction

1 | INTRODUCTION

Heart failure (HF) has a prevalence of 1%-2%, increased with aging and rising up to 10% among persons over 70 years of age. Coronary artery disease, which predisposes the heart to myocardial infarction (MI), is the main cause for systolic HF.[1] The treatment options for HF are limited, including symptom-relieving agents such as diuretics or, pharmaceuticals that modify the remodeling processes such as agents dampening renin-angiotensin system signaling or adrenergic activity. Despite the current pharmacological therapy, HF bears a high mortality rate.

HF can induce body weight loss, known as wasting or cachexia. This is accompanied by skeletal muscle wasting, which is estimated to affect at least 20% of HF patients, but the prevalence may be higher due to missed diagnoses. Muscle wasting is associated with reduced exercise capacity and poor prognosis of HF patients.[2] Muscle wasting in HF is thought to be triggered by activation of the sympathetic nervous system, the renin-angiotensin system, glucocorticoids, pro-inflammatory cytokines, and members of the transforming growth factor-β (TGFβ) family.[3] Standard drugs for HF treatment, angiotensin convertase inhibitors or beta-blockers have minor beneficial effects on reverting muscle wasting. However, anabolic agents such as testosterone and beta2-agonists represent some benefit in HF-induced muscle wasting by improving muscle function or increasing lean mass.[3]

The TGFβ family of growth factors, including activins, bone morphogenetic proteins (BMP), and growth differentiation factors (GDF), regulate cardiac physiology and pathophysiology, but their effects in the adult heart are not well known. Activin A is upregulated in the heart after MI or ischemia-reperfusion (IR) injury in experimental models[4-6] as well as in human MI.[7] Serum levels of activin A are elevated in HF and even increase with disease severity.[8] Activin A is also upregulated in T lymphocytes and in peripheral mononuclear cells in HF patients[8] and in peripheral mononuclear cells in coronary artery disease patients with stable angina.[9] Similarly, cardiac myostatin (also known as GDF8) is upregulated immediately after MI[10] and increased in human myocardium in advanced HF.[11,12] Members of the TGFβ family, activin A and myostatin, also substantially regulate skeletal muscle mass.[13,14]

Ischemic injury may be alleviated by inhibiting the signaling of these factors. For example, follistatin, an endogenous antagonist of myostatin/activin reduced IR injury in mice[5] and, in a transgenic model, the deficiency of myostatin improved cardiac function after MI.[15] Moreover, we have recently reported that systemic blockade of ACVR2B ligands protects the heart against IR injury.[6] In a recent study, inhibition of ACVR2B signaling also restored cardiac function in HF induced by aging, sarcomere mutation or pressure overload.[16] However, manipulation of these signaling pathways may also affect muscle mass. For example, cardiomyocyte-specific overexpression of myostatin induces muscle wasting in mice[17] while neutralizing antibody against myostatin reduces skeletal muscle wasting in cardiac pressure-overload-induced HF.[17] It is currently not understood how ACVR2B signaling and its inhibition contribute to cardiomyocyte function and cardiac remodeling after MI. In addition, the therapeutic potential of ACVR2B-Fc in treating skeletal muscle wasting in ischemic HF has not been addressed.

ACVR2B-Fc binds endogenous ligands activin A, myostatin (GDF8), and its close homolog GDF11 with high affinity[18] and inhibits the physiological responses of ACVR2B ligands in skeletal muscle[19-21] and heart.[6,22] ACVR2B-Fc also binds activin B, activin AB, BMP9, and BMP10, whose actions in striated muscle are less characterized.[23] In this study, we determined the effect of systemic blockade of ACVR2B ligands on the heart in post-MI remodeling and in ischemic HF as well as its effects on skeletal muscle wasting in ischemic HF.

2 | MATERIALS AND METHODS

2.1 | Myocardial infarction

Experimental protocols were approved by the Animal Use and Care Committee of the University of Oulu and by the National Animal Experiment Board (ESAVI/7250/04.10.07/2014), and all the experiments were carried out in accordance with

the guidelines of that committee and with the ethical standards laid down in the 1964 Declaration of Helsinki and its later amendments. The mice were maintained in plastic cages at a constant 21°C temperature with a 12 hours light-dark cycle and had free access to food (Teklad Global Rodent diet, Harlan Laboratories, Indianapolis, IN) and water. Immediately after operation, mice were kept in warm room at 25°C temperature overnight.

8-10 week old male C57BL/6J mice (Harlan) were subjected to myocardial infarction (MI) by ligation of the left anterior descending coronary artery (LAD) as previously described.[24,25] Sham-operated mice were subjected to the same surgical procedure without ligation of the LAD. All operations were performed under isoflurane anesthesia (Vetequip evaporiser, 2% of isoflurane with 1 L/min oxygen flow). Carprofen (Rimadyl; Zoetis, Louvain-la-Neuve, Belgium) 5 mg/kg s.c. (injection volume 0.125-0.15 mL) and buprenorphine (Vetergesic; Ceva Santé Animale, Libourne, France) 0.05 mg/kg s.c. (injection volume 0.1-0.3 mL) were administered as peri-operation analgesia. Postoperation dehydration was prevented with s.c. administration of 5% of glucose solution (injection volume 0.5-1.0 mL). All animals were monitored after the surgery and received a dose of buprenorphine (0.05 mg/kg) in the evening of the operation day. Carprofen was administered once per day and buprenorphine twice for day for three days post-MI.

2.2 | ACVR2B-Fc treatment

ACVR2B-Fc recombinant fusion protein was produced as described earlier.[21] The ectodomain of human ACVR2B was fused with a human IgG1 Fc domain and expressed in Chinese hamster ovary cells grown in suspension culture. We have verified the efficacy of ACVR2B-Fc in the heart after a single dose administered s.c.[6] and, in the skeletal muscle, after repeated dosage.[21] Experimental studies with pharmacological ACVR2B ligand blockade have been summarized in Figure 1. ACVR2B-Fc was administered as 5 mg/kg s.c. immediately after ligation of LAD and continued twice per week for 4 weeks (termed "4 wk study") or started after 4 weeks of LAD ligation and continued twice per week for 6 weeks (termed "4 + 6 wk study"). The same volume of PBS or human IgG1-Fc control was used as a vehicle control. As an additional study group, we administered ACTB-Fc, specifically blocking activin B ligand, as 5 mg/kg s.c. immediately after ligation of LAD and continued twice per week for 4 weeks (4 wk study). ACTB-Fc is a proprietary activin B ligand trap produced in CHO cells in a similar manner as ACVR2B-Fc and is based on the fusion of an N-terminally truncated human follistatin 288 sequence fused to human IgG1 Fc domain part. The dimeric ACTB-Fc ligand trap blocks activin B bioactivity in a HepG2 cell Smad2/3 assay as effectively as ACVR2B-Fc but does not block activin A and myostatin (Pasternack A, Laitinen M, Ritvos O, unpublished results). In this study, ACTB-Fc is used as a control to distinguish between activin A and B bioactivities.

In the 4 wk study, the littermates were randomly and equally divided into treatment groups to avoid any bias between the mouse litters. The person operating on the mice was blinded from treatment. Regarding 4 + 6 wk study, the hearts were evaluated by echocardiography and the ejection fraction was determined after 4 weeks of LAD ligation. The mice were divided into treatment groups with equal degrees of MI-induced injury in both groups. Ejection fractions were 22.8 ± 12.4% and 21.2 ± 7.7% at 4 weeks post-MI in the groups allocated to vehicle and ACVR2B-Fc treatments, respectively.

In addition, the expression levels of ACVR2B ligands and ACVR2 receptors in the myocardium were analyzed at 3, 5, 7, and 14 days after MI. All analysis to assess functional, histological, and other outcome were performed in a blinded manner.

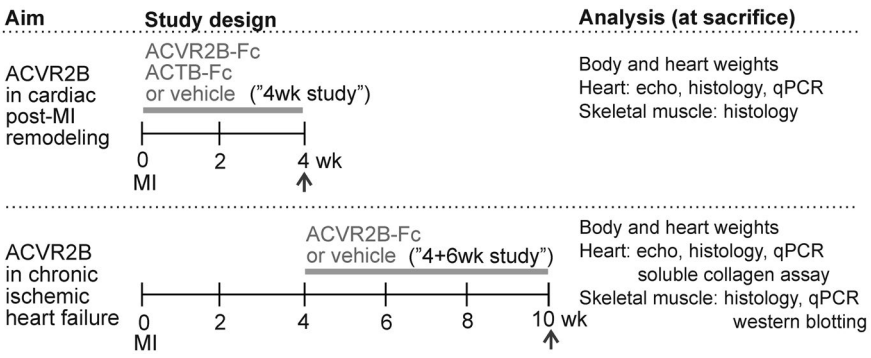

FIGURE 1 Summary of experimental MI studies with pharmacological blockade of ACVR2B signaling. In addition to experimental treatment studies, the gene expression levels of activin family members in the myocardium were analyzed at 3 d, 5 d, 7 d, 2 wk, 4 wk, and 10 wk after MI. Activin receptor 2B (ACVR2B), soluble decoy receptor ACVR2B-Fc (ACVR2B-Fc), modified follistatin-Fc protein binding activin B (ACTB-Fc), myocardial infarction (MI)

2.3 | Echocardiography

Mice were anesthetized with isoflurane and transthoracic echocardiography was performed with Vevo 2100 (Visual Sonics, Toronto, ON, Canada) high frequency, high resolution linear array ultrasound system using a MS-550D transducer (40 MHz, axial resolution 40 μm, lateral resolution 90 μm). B-mode, M-mode, mitral annular velocity-tissue Doppler images were recorded and analyzed with Vevo Workstation software 1.7 by a blinded observer.

2.4 | RNA isolation and quantitative real-time PCR

Three, 5, 7, and 14 days post-MI, and at the end of 4 wk or 4 + 6 wk treatment studies, the mice were euthanized with CO_2 and sacrificed by decapitation. The heart and quadriceps femori were then excised, the mid LV sample and mid quadriceps samples were frozen in liquid nitrogen and stored at −70°C. Thereafter, RNA was isolated with Trizol (Invitrogen, Thermo Fisher Scientific, Waltham, MA, USA) and cDNA was synthesized from 500 ng of RNA with Transcriptor First Strand cDNA synthesis kit (Roche, Basel, Switzerland). The expression levels were evaluated on an ABI Prism 7700 Sequence Detection System (Applied Biosystems, Thermo Fisher Scientific) and the oligonucleotide primer and detection probe sequences used for mRNA quantitation are presented in Table S1 and in our previous study.[6]

2.5 | Western blotting

The total protein content was extracted from the LV peri-infarct zone and mid quadriceps as described earlier[26] and the protein concentrations were determined with colorimetric protein assay (Bio-Rad Laboratories, Hercules, CA, USA). Afterward, protein samples (40 μg) were denatured at 97°C for 5 minutes and loaded on sodium dodecyl sulfate polyacrylamide gel electrophoresis (SDS-PAGE). The membranes were then incubated for 1 hour at RT in blocking buffer (Odyssey, LI-COR Biosciences, Lincoln, NE, USA) diluted into Tris-buffered saline (TBS, 50 mM Tris, 200 mM NaCl, pH 7.4). Membranes were then incubated overnight with primary antibody PGC1 C-term (Calbiochem #516557, 1:1000; Merck Millipore Sigma, Darmstadt, Germany), pERK1/2 (Thr202/Tyr204) (Cell Signaling #9106, 1:2000, Cell Signaling Technology, Danvers, MA, USA), pS6 (Ser240/244) (Cell Signaling #2215, 1:1000) or GAPDH (Merck Millipore Sigma #MAB374, 1:500 000) in blocking buffer, washed with TBS-0.05% of Tween-20, and incubated with secondary antibody (goat-anti-rabbit Alexa Fluor 680; Molecular Probes, Thermo Fisher Scientific or goat-anti-mouse IRDye 800; Rockland Immunochemicals, Pottstown, PA, USA) for 1 hour at RT. Antibody binding was detected by Odyssey Infrared Imaging System (LI-COR Biosciences) and quantified using the public domain NIH Image program (developed at the US National Institutes of Health, Bethesda, MD).

2.6 | Immunohistochemistry

After excision of the heart, a transversal section of the LV was fixed overnight in phosphate-buffered 10% of formalin (pH 7.0) and thereafter prepared as paraffin-embedded sections. Thereafter, five μm thick sections were cut from the mid-section of the heart at the level of the papillary muscles. For staining, sections were deparaffinized in xylene and dehydrated in graded ethanol series. After the quadriceps femori were fixed overnight in phosphate-buffered 10% of formalin (pH 7.0), the muscle was cut transversally from the middle, embedded in paraffin and cut in 5 μm sections.

The sections were stained with Masson's trichrome stain to visualize cardiomyocytes, cell nuclei, and fibrous tissue. Alternatively, sections were stained with 5 μg/mL of wheat germ agglutinin (WGA) Alexa Fluor 488-conjugate (Molecular Probes, Thermo Fisher Scientific). Cross-sectional myocyte cell size was quantified (Nikon NIS-Elements, Nikon, Minato, Tokyo, Japan) as an average of 50 cardiomyocytes/section obtained from five representative fields of each section (with 40× objective) from epicardial and endocardial sides of the LV. For quantification of the skeletal muscle size, paraffin-embedded sections from quadriceps femori were stained with WGA and two images per section (with 20× objective) were taken with a fluorescence microscope (Nikon Eclipse 80i). Individual cell sizes were quantified from the whole image (NIS Elements), containing approximately 100 cells/image.

Primary antibody for slow myosin heavy chain MHCI (Chemicon #MAB1628, 1:200, Merck Millipore Sigma), was used to detect the slow-twitch myocytes in the skeletal muscle. The sections were first stained with WGA, then, double-stained with MHCI and finally counterstained with DAPI. Alexa Fluor 568 goat anti-mouse IgG (A11031; Invitrogen, Thermo Fisher Scientific) was used for secondary detection. Primary antibody for PAX7 (Abcam #34360, 1:200) was used to detect satellite cells. The sections were first stained with WGA, then, double-stained with PAX7, and finally, counterstained with DAPI.

For quantifying cardiac fibrosis, the sections were stained with Picrosirius Red (Direct Red 80, Sigma, Merck Millipore Sigma) as described.[27] The sections were analyzed under the microscope with linear polarized light (Olympus BX51, Shinjuku, Tokyo, Japan) and the images were obtained from the peri-infarcted area and from the remote LV area with a color

digital camera (with 20x objective, Olympus, DP71). Red and green birefringence of collagen fibers were quantified (NIH Image Program) and averaged from multiple fields of each section representing increased interstitial fibrosis. At 4 + 6 wk study, after full fibrotic maturation and at late stage remodeling, we quantified picrosirius-stained sections with fluorescent microscope. Picrosirius red shows red fluorescence.[28] The sections were viewed under fluorescent light (with 540/25 nm filter), and imaged throughout the peri-infarcted area. The pictures were stitched together in Adobe Photoshop and total fibrosis was determined from the whole peri-infarcted LV area, which represents higher fibrosis than remote LV.

To determine adipocyte cell size, sections prepared from gonadal fat were stained for hematoxylin-eosin. Cross-sectional adipocyte cell size was quantified (Adobe Photoshop) as an average of 60 adipocytes/section obtained from four representative fields of each section (with 10× objective).

2.7 | Soluble collagen assay

To quantify the amount of soluble collagen in the myocardium, samples from LV remote area were solubilized in 0.1 mg/mL pepsin in 0.5 M acetic acid, incubated on a rotator for 24 hours at 4°C. Samples were further processed according to the manufacturer's instructions (Sircol, #S1000, Biocolor, Carrickfergus, NI, UK), and analyzed for soluble collagen with a microplate reader at 555 nm (Thermo Scientific Varioscan, Thermo Fisher Scientific).

2.8 | Statistics

Data are expressed as mean ± SD. The data were analyzed with SPSS software using Student *t* test or one-way ANOVA when appropriate, followed by Dunnett or Tukey post hoc test. When data were not normally distributed, Mann-Whitney *U* test or Kruskal-Wallis test with Bonferroni correction was used. $*P < .05$, $**P < .01$, and $***P < .001$.

3 | RESULTS

3.1 | ACVR2B ligands are differently regulated in the myocardium after MI

We first determined the time course of activation of ACVR2B ligands after MI. In IR, we have reported that myostatin and activin A are already upregulated in the myocardium at 6 hours after ischemic insult and their levels are sustained for 24 hours.[6] In MI, *Inhba* (activin A) and *Inhbb* (activin B) levels were upregulated in the myocardium during the first few days after infarction and were sustained for the first few weeks after the ischemic insult, in levels exceeding that of *Tgfb* (Tfgβ) (Figure 2A). In contrast to activin A and activin B, the levels of *Gdf8* (myostatin) were downregulated during the early days after infarction while the levels of its close homolog, *Gdf11* were not affected (Figure 2B). We then determined the levels of the main receptors binding these ligands. Here, *Acvr2b* was downregulated while *Acvr2a* also showed minor downregulation (Figure 2C). However, it should be noted that changes in the expression levels do not directly contribute to actual ACVR2B signaling but rather indicates ACVR2B signaling to be modified in MI.

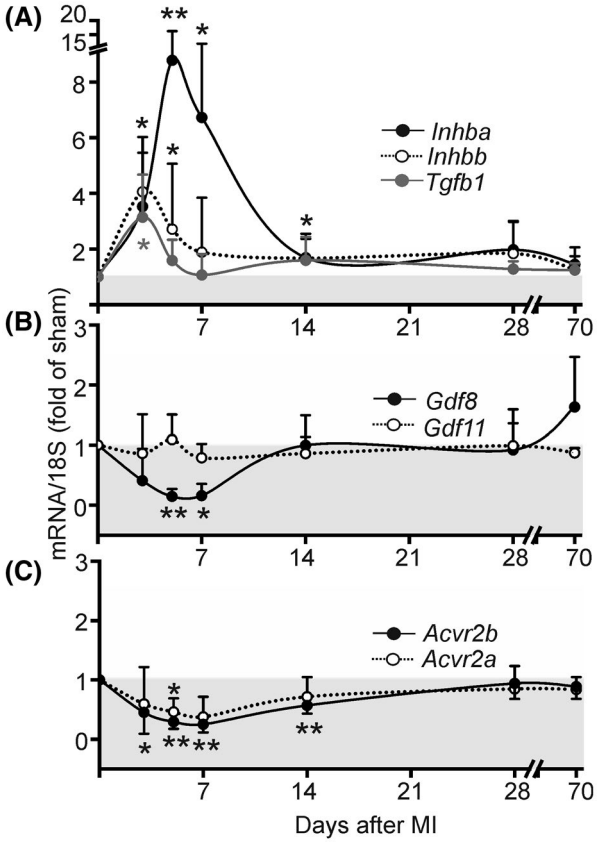

FIGURE 2 Expression of ACVR2B ligands in myocardium post-MI. MI was achieved by permanent ligation of the left anterior descending (LAD) coronary artery in mice. The time course of the expression of ACVR2B ligands was determined from LV with qPCR. The expression of Tgfb1, the main factor of TGFβ family is shown as a comparison. Additionally, the expression levels of activin type II receptors were analyzed. Levels below sham values are shown with grey. n = 5 (3 d, 5 d, 7 d, 4 wk), n = 6 (2 wk), n = 9 (10 wk). Data are presented as mean + SD. $*P < .05$, $**P < .01$ vs sham. *Inhba* (activin A), *Inbb* (activin B), *Gdf8* (myostatin)

3.2 | Systemic blockade of ACVR2B ligands does not alleviate post-MI remodeling

We then aimed to determine whether systemic blockade of ACVR2B ligands, similar to its cardioprotective effects in

transient IR model,[6] could alleviate ischemic injury, reduce cardiac remodeling and restore cardiac function after MI. Systemic blockade of ACVR2B ligands by ACVR2B-Fc was started immediately after MI and continued throughout the inflammatory and reparative phases (4 wk study). Complementary to ACVR2B-Fc, which blocks ACVR2B ligands activin A, activin B, myostatin, and GDF11, we treated an additional group of mice with an inhibitor, which induces systemic blockade of activin B ligand specifically (ACTB-Fc).

The MI model is associated with approximately 30% mortality rate,[24] mainly caused by LV rupture during 3-7 days post-MI. In our 4 wk study, where treatments were started immediately after MI, 7 out of 24 MI-operated mice died in the first few days after infarction. In more detail, 5/10 mice in the vehicle-treated MI group, 7/9 mice in the ACVR2B-Fc-treated MI group and 5/5 mice in the ACTB-Fc-treated mice survived until end of 4 wk study (Figure S1). However, survival was not significantly different in comparison to the vehicle-treated MI group.

When monitoring cardiac function 4 weeks post-MI by echocardiography, neither ACVR2B-Fc nor ACTB-Fc had an effect on cardiac systolic function or LV dimensions (Figure 3A, Table S2). ACVR2B-Fc or ACTB-Fc did not affect cardiac mass, cardiomyocyte size (Figures 3B and S1) or fibrosis (Figure 3C). ACVR2B-Fc did not affect gene expression of hypertrophic, fibrotic or angiogenetic factors (Figure S1). However, ACVR2B-Fc upregulated, although not significantly, factors associated with remodeling and fibrosis, such as *Il6* (Figure S1, $P = .09$). ACTB-Fc also slightly upregulated *Fgf2* (Figure S1, $P = .06$). ACVR2B-Fc or ACTB-Fc did not cause compensatory upregulation of ACVR2B ligands or type II receptors (Figure S1).

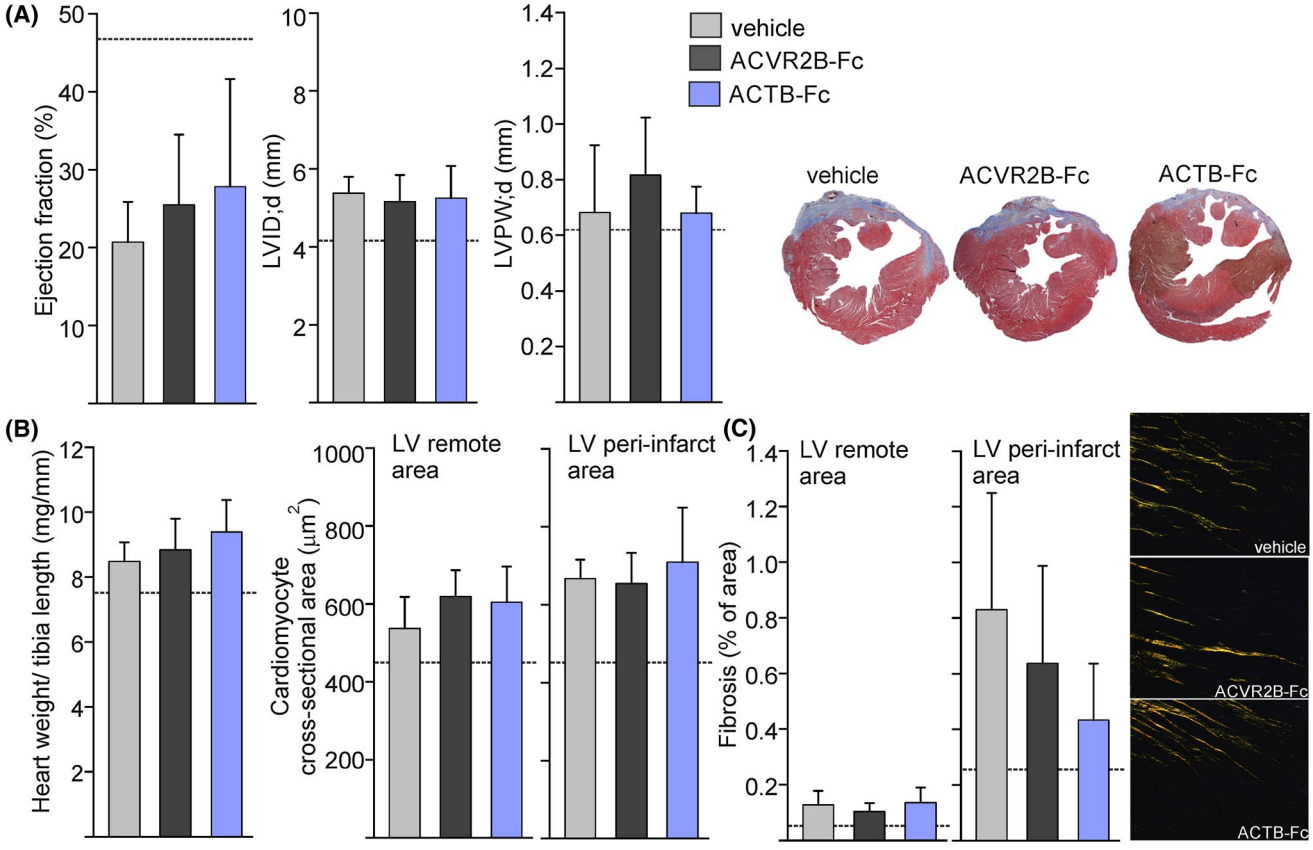

FIGURE 3 ACVR2B-Fc or ACTB-Fc do not alter post-MI remodeling. Mice were treated with vehicle (grey columns), with a soluble decoy receptor ACVR2B-Fc (ACVR2B-Fc, black columns) or with a modified follistatin-Fc protein binding activin B (ACTB-Fc, blue columns). Treatment was started immediately after permanent ligation of the left anterior descending (LAD) coronary artery and continued for 4 weeks (4 wk study). A, As determined with echocardiography, neither ACVR2B-Fc nor ACTB-Fc affected the cardiac function, ventricular remodeling (left ventricular diameter in diastole, LVID;d) or hypertrophy (LV posterior wall thickness, LVPW;d) in MI mice (complementary echocardiography data in Table S2). Representative pictures of Masson trichrome stained heart sections, cut horizontally. B, ACVR2B-Fc or ACTB-Fc did not induce cardiac hypertrophy. C, ACVR2B-Fc or ACTB-Fc did not affect cardiac fibrosis as determined with picrosirius red stain from cardiac sections. Representative images of picrosirius red-stained collagen fibers in cardiac sections pictured from the peri-infarcted area under polarized light. ACVR2B-Fc or ACTB-Fc did not affect genes related to cardiac hypertrophy, fibrosis or angiogenesis (Supplementary data in Figure S1). Sham values are shown as a dotted line. n = 5, 7, 5 (A, B), n = 3, 4, 3 (B, peri-infarcted area), n = 3, 4, 4, (C). Data are presented as mean + SD

3.3 | Systemic blockade of ACVR2B ligands does not improve cardiac function in ischemic heart failure

Next, we aimed to study whether ACVR2B-Fc could improve cardiac function when administered after established ischemic HF. ACVR2B-Fc treatment was started 4 weeks after MI and continued for 6 weeks (4 + 6 wk study). ACVR2B-Fc treatment started at chronic stage post-MI did not affect cardiac systolic function or LV dimensions (Figure 4A, Table S3). Furthermore, ACVR2B-Fc did not significantly provoke MI-induced cardiac hypertrophy during the 6-week treatment (Figure 4B). ACVR2B-Fc slightly reduced cardiac fibrosis in the late-remodeling stage, but this was not statistically significant (Figure 4C, $P = .057$). We determined the expression levels of multiple genes associated with cardiac hypertrophy, fibrosis, angiogenesis, cardiogenesis, migration, contractility, and metabolism (Figure S2). We detected ACVR2B-Fc to upregulate *Tnf* (Tnfα) ($P < .05$) and *Angpt2* (angiopoietin 2) ($P < .05$) and a similar trend was detected already in the 4 wk study (Figure S1). Interestingly, ACVR2B-Fc downregulated *Ddit4* (Redd1) ($P < .05$), DNA damage-inducible transcript, which regulates cell growth and survival (Figure S2). In addition, ACVR2B-Fc upregulated Pgc1α4, an alternative splice variant of the *Ppargc1a* (Pgc1α) gene ($P < .01$), associated with physiological hypertrophy in striated muscle.[29] ACVR2B-Fc also substantially downregulated the expression of *Ccl21* ($P < .001$), a chemokine and the ligand for CCR7 receptor, associated with immunological responses and tissue remodeling but the function in the heart remains mostly unknown. The expression of CCL21 is increased in the heart and serum during HF, and its high levels are associated with increased mortality in patients with HF.[30,31] The downregulation of *Ccl21* in the current study, however, did not contribute to any notable changes in cardiac homeostasis during ischemic HF.

When treating sham mice, ACVR2B-Fc downregulated the expression of *Nppa* (atrial natriuretic peptide) ($P < .01$) and Acta1 (skeletal muscle actin-α) ($P < .05$). Although *Lox* was slightly elevated, collagen deposition was not significantly increased by ACVR2B-Fc in sham mice (Figure S2).

3.4 | Systemic blockade of ACVR2B ligands other than activin B increases skeletal muscle size post-MI and in ischemic heart failure

We then aimed to study whether ACVR2B-Fc could reduce skeletal muscle loss in HF-induced muscle wasting. In 4 wk study, ACVR2B-Fc treatment in MI mice increased both bodyweight and skeletal muscle size whereas the blocking of activin B had no effects (Figure 5A). ACVR2B-Fc also induced physiological changes outside the musculature, which were not obtained by blocking only activin B. ACVR2B-Fc-induced splenomegaly and reduced fat mass in MI mice, determined by reduced adipocyte size (Figure S3). In addition to altering adipose phenotype, myostatin deficient mice have greater insulin sensitivity.[32,33] In line with this, ACVR2B-Fc lowered blood glucose levels in MI mice, although not statistically significantly ($P = .08$).

Similarly, 6 wk treatment with ACVR2B-Fc (4 + 6 wk study) increased bodyweight in ischemic HF mice but not to same extent as their sham counterparts (Figure 5B). ACVR2B-Fc already increased bodyweight after 1 week of treatment, both in the sham and MI mice (Figure 5B). To ensure that this was due to muscle hypertrophy, we quantified the size of muscle fibers in the quadriceps skeletal muscle and observed that ACVR2B-Fc increased the mean myofiber size in this muscle group (Figure 5C). When examined in more detail, MI increased the proportion of small myofibers, which suggests that muscle wasting was present in our model of ischemic HF. Furthermore, ACVR2B-Fc decreased the proportions of small myofibers while also increasing the proportion of larger myofibers (Figure 5C). Increased muscle fiber size by ACVR2B-Fc was associated with increased mTORC1 signaling as marked by an increased phosphorylation of pS6 whereas phosphorylation of ERK was not affected (Figure 5D). ACVR2B-Fc lowered the protein level of PGC1α in skeletal muscle (Figure 5D) and its transcript levels (Figure S4) suggesting metabolic alterations in addition to hypertrophy. This was accompanied by ACVR2B-Fc lowering the gene expression of *Myh7* (MHCβ) while no changes in the proportion of MHCI slow-twitch myofibers were detected (Figure 5E). ACVR2B-Fc did not increase activation of satellite cells (Figure S4).

In addition to lowering *Ppargc1a* (Pgc1α1) expression, ACVR2B-Fc downregulated *Pfkm* gene expression (Figure S4) in skeletal muscle while upregulating *Cited4* expression (Figure 5E). ACVR2B-Fc nonsignificantly downregulated atrogenes *Fbxo32* (Atrogin1, $P = .08$) and *Trim63* (Murf1, $P = .07$) (Figure S4), which was accompanied by reduced lipidated LC3 (LC3II) as a marker of autophagy (Figure 5F). ACVR2B-Fc did not affect the expression levels of ACVR2B ligands *Inhba*, *Inhbb*, *Tgfb1* or receptors *Acvr2a*, *Acvr2b* or BMP receptor *Bmpr2* (Figure S4). However, ACVR2B-Fc increased the expression levels of *Gdf11* in MI mice and both *Gdf11* and *Gdf8* in sham mice (Figure S4). This suggests that there is a compensatory increase of these anti-hypertrophic factors after ACVR2B-Fc-induced muscle hypertrophy. Since BMPs can also regulate muscle mass,[34] we determined the levels of BMPs in MI mice and in response to ACVR2B-Fc treatment. While other BMPs were not affected, MI induced slight upregulation of *Gdf6* (Bmp13) (Figure S4, $P = .06$) in skeletal muscle. In the heart, MI reduced the expression of *Bmp7* and similarly to skeletal muscle, increased the expression of *Gdf6* (Bmp13) (Figure S4, $P < .05$). ACVR2B-Fc, however, did not affect BMP levels in skeletal muscle or in the heart.

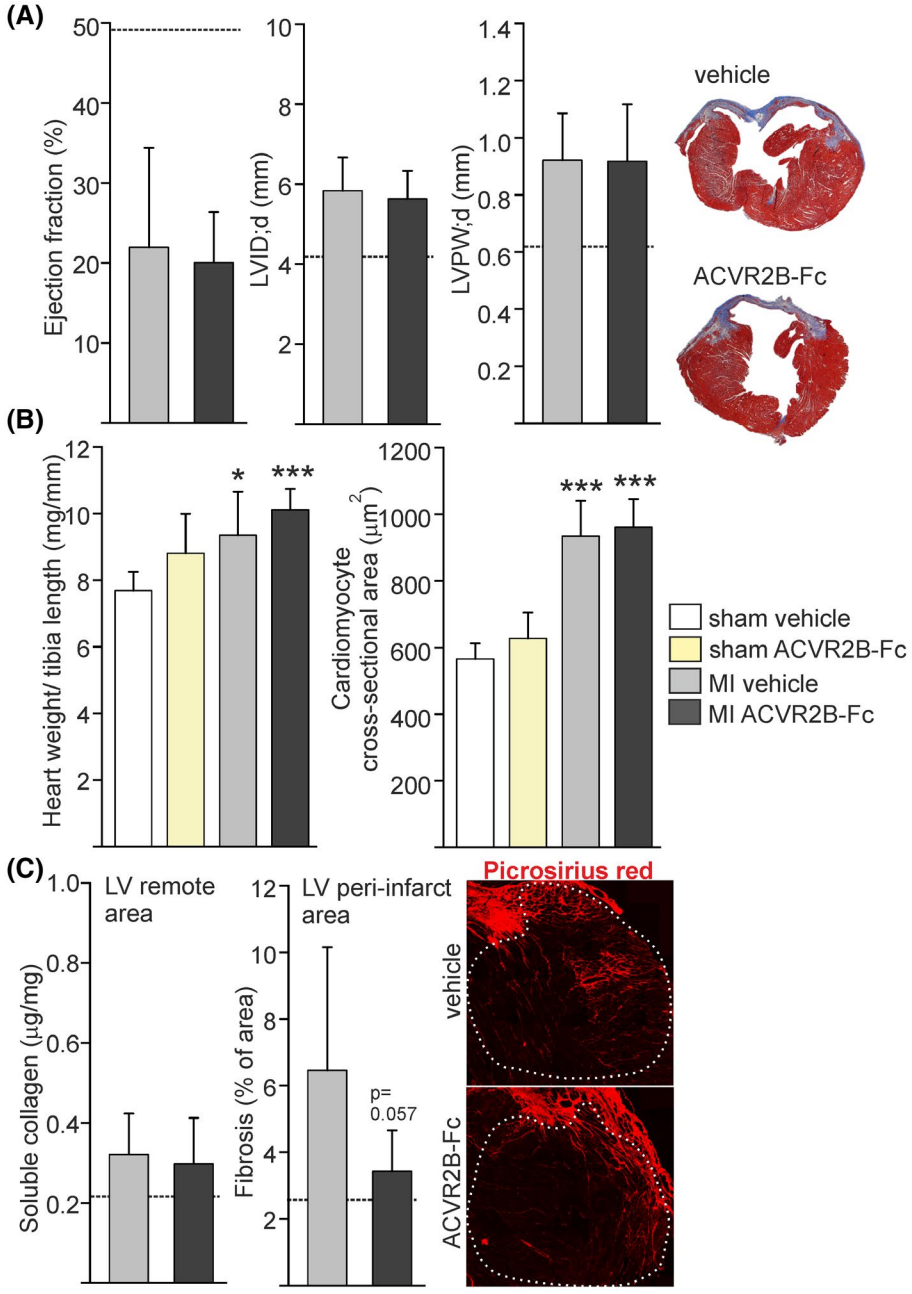

FIGURE 4 ACVR2B-Fc does not modify cardiac function, hypertrophy or fibrosis in ischemic heart failure. Mice were treated with vehicle (grey columns) or with a soluble decoy receptor ACVR2B-Fc (ACVR2B-Fc, black columns). Treatment was started 4 weeks after permanent ligation of the left anterior descending (LAD) coronary artery and continued for 6 weeks (4 + 6 wk study). A, When evaluated using echocardiography, ACVR2B-Fc did not affect the cardiac function, ventricular remodeling (left ventricular diameter in diastole, LVID;d) or hypertrophy (LV posterior wall thickness, LVPW;d) in MI mice (complementary echocardiography data in Table S3). Representative pictures of Masson trichrome stained heart sections cut horizontally. B, ACVR2B-Fc did not induce cardiac hypertrophy. In comparison, heart weight to body weight ratios and cardiomyocyte cross-sectional area shown for sham-operated vehicle-treated (white columns) and ACVR2B-Fc-treated (yellow columns) mice. C, ACVR2B-Fc did not affect cardiac fibrosis as determined with picrosirius red stain from cardiac sections. Representative images of picrosirius red-stained collagen fibers in cardiac sections pictured from the peri-infarcted area under fluorescent light. Complementary data on ACVR2B-Fc affected genes in myocardial hypertrophy, fibrosis, angiogenesis, cardiogenesis, and metabolism in Figure S2. Sham values are shown as a dotted line. n = 8, 9 (A, C), n = 5, 4, 8, 9 (B). Data are presented as mean + SD. *$P < .05$, ***$P < .001$ vs sham

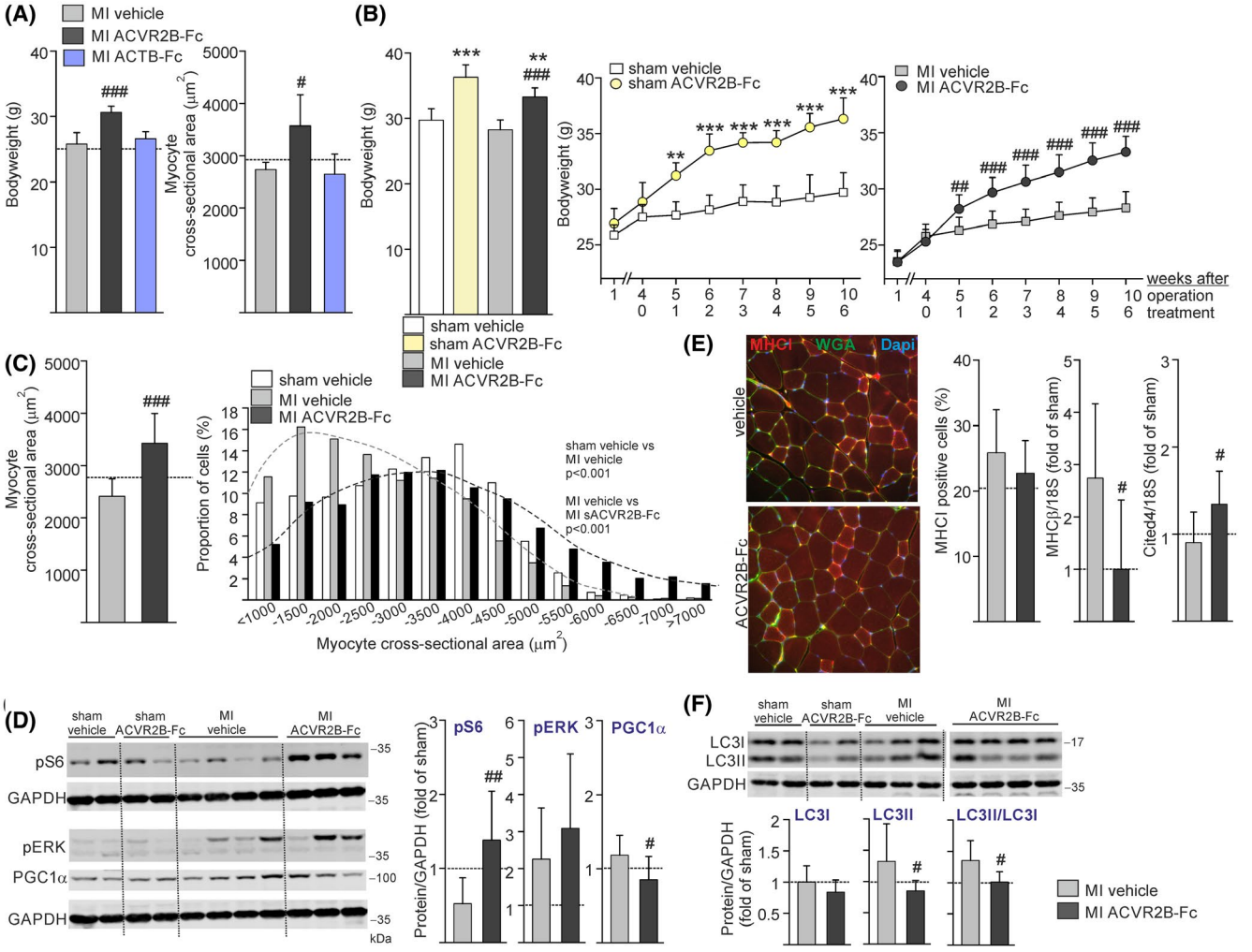

FIGURE 5 ACVR2B-Fc increases skeletal muscle hypertrophy post-MI and in ischemic heart failure. MI was induced by permanent ligation of the left anterior descending (LAD) coronary artery. Vehicle, ACVR2B-Fc or ACTB-Fc treatment was started immediately after operation (4 wk study, A) or 4 weeks after the operation (4 + 6 wk study, B-F). A, ACVR2B-Fc treatment increased bodyweight and skeletal muscle size post-MI while ACTB-Fc had no effect on skeletal muscle hypertrophy. B, ACVR2B-Fc treatment increased bodyweight in ischemic HF. Data for sham-operated vehicle or ACVR2B-Fc-treated mice shown as comparison. C, ACVR2B-Fc treatment increased mean skeletal muscle size in the quadriceps muscle of animals with ischemic HF. In addition, ACVR2B-Fc shifted the distribution of cross-sectional areas toward larger cell size, reversing MI-induced muscle wasting (grey and black scatter lines visualizing the distributions). D, ACVR2B-Fc increased the phosphorylation of S6, an indicator of mTOR signaling while phosphorylation of ERK was not affected. ACVR2B-Fc lowered the protein level of PGC1α in skeletal muscle suggesting metabolic alterations in addition to hypertrophy. E, As analyzed from MHCI double stain with wheat germ agglutinin, ACVR2B-Fc did not significantly reduce the proportion of MHCI slow-twitch myocytes in the quadriceps but ACVR2B-Fc lowered the expression of MHCβ. This was accompanied by upregulation of Cited4. F, ACVR2B-Fc reduced autophagy in the quadriceps muscle. Complementary data on ACVR2B-Fc affected genes in skeletal muscle metabolism and atrophy represented in Figure S4. Sham values are shown as a dotted line. n = 5, 7, 5 (A), n = 5, 4, 8, 9 (B, D), n = 5, 7, 9 (C, E immunostaining, F), n = 6, 7 (E, qPCR). Data are presented as mean ± SD. $^{**}P < .01$, $^{***}P < .001$ vs sham, $^{\#}P < .05$, $^{\#\#}P < .01$, $^{\#\#\#}P < .001$ vs MI vehicle

4 | DISCUSSION

4.1 | ACVR2B-Fc promotes skeletal muscle hypertrophy but has no effect on cardiac function or remodeling post-MI or in ischemic heart failure

Daily administration of follistatin, the endogenous inhibitor of activins and myostatin for 4 weeks after experimental MI, decreases sympathetic remodeling and inflammatory activation, accompanied by sustained cardiac function.[35] In our previous study, we found that ACVR2B-Fc reduced transient ischemia-reperfusion injury in the heart.[6] In the current study, we further investigated whether the blockade of ACVR2B signaling alleviates post-MI remodeling. In order to investigate whether the effects of ACVR2B-Fc may be in part through activin B, we also administered a novel blocker for activin B. We observed that, with systemic blockade of

ACVR2B ligands, we did not detect a reduction in inflammation or preservation of cardiac function in permanent MI, even though the treatment was started immediately after MI or administered at the time point for chronic heart failure. In a pressure overload model, blockade of ACVR2 signaling improves systolic function even if started 2 weeks after induction of pressure overload.[16] In this study, ACVR2B-Fc lowered the expression of ANP and skeletal α-actin in sham mice, but this was not able to generate cardioprotection in ligation model of MI.

ACVR2 ligands bind to activin receptor 2A and 2B (ACVR2A and ACVR2B),[23,36] which in turn activate type I receptors such as activin receptor-like kinases (ALK) ALK4 and ALK5, activating downstream molecule SMAD2/3.[37,38] SMADS regulate myogenic genes that are involved in cellular hypertrophy, proliferation or differentiation.[39] In addition to SMAD2/3 signaling, ACVR2 ligands also signal through noncanonical pathways to regulate cardiomyocyte growth by upregulation of atrophy-related atrogenes or autophagy genes resulting in proteasome-dependent muscle protein degradation and decreased muscle protein synthesis.[38]

We found that ACVR2B-Fc reversed muscle loss and increased skeletal muscle hypertrophy in infarcted mice. This was accompanied by increased mTOR signaling as determined by increased phosphorylation of ribosomal protein S6, as described previously in healthy and cachectic mice.[19,21] In addition, ACVR2B-Fc increased the gene expression of Creb binding protein (CBP)/p300-interacting transactivator with ED-rich carboxy-terminal domain-4 (Cited4), a transcription factor involved in physiological hypertrophy and increased mTOR signaling in cardiac muscle.[40,41] ACVR2B-Fc also upregulates Cited4 after IR injury in the heart,[6] but we did not detect this after prolonged use of ACVR2B-Fc in the postischemic heart.

ACVR2B-Fc-induced skeletal muscle hypertrophy was not accompanied by increased phosphorylation of ERK. ACVR2B-Fc was previously shown to restore ERK phosphorylation in cancer cachexia and to prevent skeletal muscle atrophy.[20] We also found ACVR2B-Fc-induced skeletal muscle hypertrophy was associated with a trend of reduced atrogene expression, namely Atrogin-1 and MuRF1, which was described before when ACVR2B-Fc reduced muscle wasting in cancer cachexia.[20,42] This was accompanied by a reduction of the autophagosomal form of LC3 and the ratio of autophagy-induced LC3II in the membrane versus the cytosolic LC3I form, which suggests decreased autophagosome formation and/or increased autophagosome turnover/clearance. To conclude, ACVR2B-Fc-induced hypertrophy in skeletal muscle in mice with ischemic HF include mechanisms of physiological hypertrophy accompanied by increased mTOR signaling and reduction of atrogenes/autophagy. This suggests that the hypertrophy occurs in a conventional manner previously described for ACVR2B blockade. Furthermore, as ACVR2B-Fc did not increase proliferation of satellite cells, similar to described before,[43] it appears that ACVR2B-Fc thus blocks the direct effects of ACVR2B ligands on muscle.

Cardiac overexpression of myostatin induces muscle wasting while myostatin blocking antibody reduces skeletal muscle wasting in pressure-overload-induced heart failure.[17] Although we did not detect an effect of ACVR2B-Fc on the myocardium, ACVR2B-Fc could alter cardiokine secretion from the heart, regulating skeletal muscle function. To confirm the efficacy of ACVR2B-Fc in addition to increased skeletal muscle hypertrophy, we also detected other physiological effects of ACVR2B blockade, that is, reduction of adipose tissue, splenomegaly, and reduction of blood glucose in MI mice.

The limitation of the study is that skeletal muscle masses were not weighed. In addition, we did not monitor skeletal muscle function. However, based on increased body weight, increased myofiber cross-sectional area and increased mTOR signaling in skeletal muscle, we suggest that blockade of ACVR2B signaling attenuates muscle wasting in ischemic HF. This is significant as maintenance of skeletal muscle mass can prevent common pathological conditions.[44] Muscle mass serves as a reservoir for amino acids to maintain protein synthesis in vital organs, and loss of muscle mass is an important factor for survival in HF.[2]

4.2 | ACVR2B-Fc induces metabolic modification in skeletal muscle in ischemic heart failure

Myostatin deficiency or treatment with ACVR2B-Fc downregulates the expression of MHCβ in skeletal muscle. This is accompanied by a reduction in expression of genes involved in oxidative phosphorylation.[45] Similarly, we found ACVR2B-Fc to downregulate MHCβ and a key metabolic gene PGC1α1 at both the gene and protein level in the quadriceps muscle of mice with HF. Metabolic alterations by ACVR2B-Fc have been linked to increased muscle fatigability, especially in dystrophic mice.[46] On the contrary, when given to healthy mice, ACVR2B-Fc impaired mitochondrial function but did not compromise the bioenergetics status during muscle activity.[47] In the current study, we did not analyze the endurance capacity of MI mice but skeletal muscle hypertrophy and its metabolic changes did not affect cardiac structure or function. If it caused increased skeletal muscle fatigability, this would probably lead to increased cardiovascular stress, worsening of cardiac remodeling with increased extracellular matrix production and an increased expression of fetal gene program factors. By analyzing a variety of genes controlling cardiac function and remodeling processes, we did not encounter an indication of worsening the heart failure status.

Contrary to downregulation of PGC1α1 in skeletal muscle, ACVR2B-Fc upregulated PGC1α4 in the heart. A PGC1α4 isoform that results from alternative promoter usage and splicing of the primary PGC1α transcript induces robust skeletal muscle hypertrophy without regulating metabolic effects such as oxidative phosphorylation similar to what the PGC1α1 isoform does.[29] As there was no clear benefit of ACVR2B-Fc treatment on cardiac function or remodeling, the upregulation of PGC1α4 probably reflects the minor hypertrophic effect of ACVR2B-Fc in the heart. We did not detect that ACVR2B-Fc alters the expression of genes involved in oxidative phosphorylation or glycolysis. This suggests that there has been no conversion of cardiomyocyte energy production to glycolytic metabolism after prolonged ACVR2B-Fc treatment, which could be detrimental to a failed heart.[48] In addition, ACVR2B-Fc did not change the expression of genes involved in contractility and, in line with this, there was no change in cardiac systolic function, unlike recently described in nonischemic heart failure models.[16] To conclude, ACVR2B-Fc induces metabolic changes in skeletal muscle by possibly restricting mitochondrial function but not contributing to myopathy while, at the same time, upregulating PGC1α4, an alternative splicing product in the heart.

It has been reported that myostatin deficiency increases LV diameter and decreases systolic function, inducing eccentric cardiac hypertrophy.[49] Inactivation of myostatin in cardiomyocytes leads to increased glycolysis and glycogen accumulation, substantial cardiac hypertrophy and heart failure.[50] This was even associated with >25% mortality in healthy mice just 10 days after induction of myostatin deficiency. In our study ACVR2B-Fc, blocking systemic myostatin signaling, did not cause cardiac hypertrophy or any signs of worsening of HF. We observed no lethality after one week following the induction of MI.

4.3 | Contribution of ACVR2B ligands into skeletal muscle wasting in heart failure

In addition to myostatin, other ACVR2B ligands may contribute to HF. Recently, activin A was suggested as the primary culprit for cardiac dysfunction in HF models, as adenoviral delivery of activin A impaired cardiac function even in healthy mice.[16] However, the function of the pleiotropic factor, GDF11, in the heart and skeletal muscle is still controversial.[51] Thus, we found it of high interest to block activin A, myostatin, and GDF11 signaling with ACVR2B-Fc, in post-MI remodeling and ischemic HF to better understand the role of ACVR2B signaling in cardiovascular diseases. Activin B has been shown to modulate inflammation and fibrotic activation in kidney IR injury or in kidney transplantation.[52,53] As activin B was upregulated in the heart post-MI and its effects in the heart are not known, we used an additional setting to specifically block activin B. Blockade of activin B may distinguish the inflammatory component of ACVR2B signaling from the cell viability/growth regulating effects by activin A, myostatin, and GDF11. In the current study, however, systemic blockade of activin B, similarly to ACVR2B-Fc, did not alleviate post-MI remodeling. Unlike ACVR2B-Fc, which induced skeletal muscle hypertrophy, systemic blockade of activin B did not increase muscle size.

Similarly to myostatin, GDF11 expression is increased during aging and inhibits muscle regeneration,[54] while its cachectic effects could be reversed by blockade of ACVR2A/ACVR2B.[55] Furthermore, while exogenous GDF11 reduces cardiac hypertrophy and fibrosis after pressure overload, it also induces severe cachexia, which even leads to increased death.[56] Although we did not detect changes in the expression level of GDF11, we cannot rule out that ACVR2B-Fc could have mediated skeletal muscle hypertrophy partly by blocking effects of GDF11. In zebrafish, activin A has been shown to promote heart regeneration by acting as a cardiomyocyte mitogen after cardiac injury,[57] and provides an outcome opposite to that of myostatin. As likely expected in infarcted adult mammalian heart, we did not detect an effect of ACVR2B-Fc on genes involved in cardiac stem cell activation, cardiomyogenesis or cardiac differentiation.

4.4 | ACVR2B signaling in post-MI inflammation, cardiac remodeling, and fibrosis

Myostatin deficiency not only increases skeletal muscle mass, but also reduces cardiac fibrosis and improves cardiac function in senescent mice.[58]

In a conditional mouse model, increased expression of myostatin in cardiomyocytes induces interstitial fibrosis and impairs cardiac contractility.[59] Furthermore, inhibition of myostatin by ACVR2B-Fc reverses fibrosis in the skeletal muscle of dystrophic mice by increasing fibroblast apoptosis.[60] Since activins are suggested to contribute to inflammatory and fibrotic diseases,[61] we also assessed the effect of the blockade of ACVR2B ligands in postmyocardial remodeling and in ischemic HF.

Infarction is followed by acute inflammatory response (up to 4 days post-MI), involving the recruitment of innate and adaptive immune cells into the injured area. However, other sets of leukocytes and activation and differentiation of fibroblasts, also involving angiogenesis, contributes to resolution of inflammation, and wound repair (days 4-14 post-MI). Thereafter, fibrosis is completed by a scar maturation phase and, late cardiac remodeling, possibly involving chronic inflammation which occurs weeks to months after MI.[62] Considering the view that ACVR2B ligands can regulate a variety of cell types affected in the infarcted heart, it is surprising how small the effect of long-term blockade of ACVR2B

signaling has on post-MI remodeling. ACVR2B-Fc increased the expression of the inflammatory cytokine TNFα, which is known to contribute to reduced contractility, cardiomyocyte hypertrophy, and fibrosis.[63] However, the upregulation of TNFα did not compromise cardiac function and there was rather a trend to reduced fibrosis.

4.5 | Therapeutic aspects of ACVR2B-Fc in the treatment of heart failure-induced muscle wasting

Systemic blockade of ACVR2B ligands in mice has been shown to revert chemotherapy-[20,22] and cancer-induced muscle wasting,[19,42] and to alleviate sarcopenia in dystrophic mice.[21,64,65] In addition, ACVR2B-Fc has been reported to reduce tumor-induced splenomegaly.[19] While MI did not induce spleen growth itself, 4 or 6 week treatment with ACVR2B-Fc-induced substantial splenomegaly both in healthy and in infarcted mice. This increase in spleen size is comparable to that obtained from administration of granulocyte colony stimulating factor,[66] a hematopoietic mobilization agent which has side effects that include severe splenomegaly and even spleen rupture. The induction of splenomegaly by ACVR2B-Fc is probably due to blockade of GDF11, since GDF11 is known to be involved in hematopoiesis by controlling erythrocyte maturation.[51] To overcome these possible side effects, systemic blockade of ACVR2B ligands, to treat muscle wasting, should preferably be replaced by more selective agents such as specific antibodies to activin A or myostatin,[13] thus, not affecting GDF11.

Drugs in preclinical and early stage clinical development for the treatment of HF display a variety of targets. They are directed to inflammation, hyperglycemia, cardiac ion channels, diuresis, metabolism, neurohumoral activity, vasodilatation and, ventricular remodeling. Pirfenidone, an inhibitor for TGFβ1 is in Phase 2 clinical trials to evaluate its efficacy to restrict cardiac remodeling and fibrosis in patients whom have HF with preserved ejection fraction.[67] Considering that ACVR2B ligands target many of the abovementioned physiological functions, it was rather unexpected to not detect a significant benefit of ACVR2B-Fc treatment for the heart in ischemic HF. Importantly, even though systemic blockade of ACVR2B ligands after MI is not beneficial to the heart, it is not detrimental for the healthy or injured heart when treating skeletal muscle wasting.

To conclude, our data show that systemic blockade of ACVR2B ligands did not affect cardiac hypertrophy, fibrosis or cardiac function in post-MI remodeling phase and ischemic HF. ACVR2B-Fc increased skeletal muscle hypertrophy in infarcted mice, which did not compromise cardiac function or worsen HF pathology. Despite its possible side effects on hematopoietic system, ACVR2B-Fc could be a therapeutic for HF-induced muscle wasting as ACVR2B-Fc prevented chronic MI-induced skeletal muscle wasting. It remains to be elucidated whether dual blockade of ACVR2A/ACVR2B by bimagrumab, which provides full anabolic response in skeletal muscle,[36] could offer benefit for the infarcted heart.

ACKNOWLEDGMENTS

We thank Marja Arbelius, Sirpa Rutanen, and Kirsi Salo (University of Oulu) for excellent technical assistance. This work was supported by research funding from the Academy of Finland grant No: 268505 (JM), grant No: 275922 (JJH), and grant No: 297094 (RK) and the Finnish Foundation for Cardiovascular Research (JM, RK).

CONFLICT OF INTEREST

Zoltán Szabó, Laura Vainio, Ruizhu Lin, Julia Swan, Juha Hulmi, Lea Rahtu-Korpela, Raisa Serpi, Mika Laitinen, Arja Pasternack, Olli Ritvos, Risto Kerkelä, and Johanna Magga declare that they have no conflicts of interest. The manuscript does not contain clinical studies or patient data.

AUTHOR CONTRIBUTIONS

R. Kerkelä and J. Magga designed the study. Z. Szabó, L. Vainio, R. Lin, J. Swan, L. Rahtu-Korpela, R. Serpi, and J. Magga performed research. Z. Szabo, L. Vainio, R. Lin, J. Swan, L. Rahtu-Korpela, R. Kerkelä, and J. Magga analyzed data. J. Magga wrote the manuscript. J. Swan, J.J. Hulmi, R. Serpi, O. Ritvos, and R. Kerkelä critically revised the manuscript. J.J. Hulmi, M. Laitinen, A. Pasternack, and O. Ritvos designed, produced, and tested pharmacological agents and participated in design of the study. All authors have read and approved final manuscript.

REFERENCES

1. McMurray JJ. Clinical practice. Systolic heart failure. *N Engl J Med*. 2010;362:228-238.
2. Fulster S, Tacke M, Sandek A, et al. Muscle wasting in patients with chronic heart failure: results from the studies investigating co-morbidities aggravating heart failure (SICA-HF). *Eur Heart J*. 2013;34:512-519.
3. von Haehling S, Ebner N, Dos Santos MR, Springer J, Anker SD. Muscle wasting and cachexia in heart failure: mechanisms and therapies. *Nat Rev Cardiol*. 2017;14:323-341.
4. Oshima Y, Ouchi N, Shimano M, et al. Activin A and follistatin-like 3 determine the susceptibility of heart to ischemic injury. *Circulation*. 2009;120:1606-1615.
5. Chen Y, Rothnie C, Spring D, et al. Regulation and actions of activin A and follistatin in myocardial ischaemia-reperfusion injury. *Cytokine*. 2014;69:255-262.
6. Magga J, Vainio L, Kilpio T, et al. Systemic blockade of ACVR2B ligands protects myocardium from acute ischemia-reperfusion injury. *Mol Ther*. 2019;27:600-610.
7. Miyoshi T, Hirohata S, Uesugi T, et al. Relationship between activin A level and infarct size in patients with acute myocardial infarction undergoing successful primary coronary intervention. *Clin Chim Acta*. 2009;401:3-7.

8. Yndestad A, Ueland T, Oie E, et al. Elevated levels of activin A in heart failure: potential role in myocardial remodeling. *Circulation*. 2004;109:1379-1385.
9. Smith C, Yndestad A, Halvorsen B, et al. Potential anti-inflammatory role of activin A in acute coronary syndromes. *J Am Coll Cardiol*. 2004;44:369-375.
10. Castillero E, Akashi H, Wang C, et al. Cardiac myostatin upregulation occurs immediately after myocardial ischemia and is involved in skeletal muscle activation of atrophy. *Biochem Biophys Res Commun*. 2015;457:106-111.
11. George I, Bish LT, Kamalakkannan G, et al. Myostatin activation in patients with advanced heart failure and after mechanical unloading. *Eur J Heart Fail*. 2010;12:444-453.
12. Gruson D, Ahn SA, Ketelslegers JM, Rousseau MF. Increased plasma myostatin in heart failure. *Eur J Heart Fail*. 2011;13:734-736.
13. Latres E, Mastaitis J, Fury W, et al. Activin A more prominently regulates muscle mass in primates than does GDF8. *Nat Commun*. 2017;8:15153.
14. McPherron AC, Lawler AM, Lee SJ. Regulation of skeletal muscle mass in mice by a new TGF-beta superfamily member. *Nature*. 1997;387:83-90.
15. Lim S, McMahon CD, Matthews KG, Devlin GP, Elston MS, Conaglen JV. Absence of myostatin improves cardiac function following myocardial infarction. *Heart Lung Circ*. 2018;27(6):693-701.
16. Roh JD, Hobson R, Chaudhari V, et al. Activin type II receptor signaling in cardiac aging and heart failure. *Sci Transl Med*. 2019;11:eaau8680.
17. Heineke J, Auger-Messier M, Xu J, et al. Genetic deletion of myostatin from the heart prevents skeletal muscle atrophy in heart failure. *Circulation*. 2010;121:419-425.
18. Sako D, Grinberg AV, Liu J, et al. Characterization of the ligand binding functionality of the extracellular domain of activin receptor type IIb. *J Biol Chem*. 2010;285:21037-21048.
19. Nissinen TA, Hentila J, Penna F, et al. Treating cachexia using soluble ACVR2B improves survival, alters mTOR localization, and attenuates liver and spleen responses. *J Cachexia Sarcopenia Muscle*. 2018;9:514-529.
20. Nissinen TA, Degerman J, Rasanen M, et al. Systemic blockade of ACVR2B ligands prevents chemotherapy-induced muscle wasting by restoring muscle protein synthesis without affecting oxidative capacity or atrogenes. *Sci Rep*. 2016;6:32695.
21. Hulmi JJ, Oliveira BM, Silvennoinen M, et al. Muscle protein synthesis, mTORC1/MAPK/Hippo signaling, and capillary density are altered by blocking of myostatin and activins. *Am J Physiol Endocrinol Metab*. 2013;304:E41-E50.
22. Hulmi JJ, Nissinen TA, Rasanen M, et al. Prevention of chemotherapy-induced cachexia by ACVR2B ligand blocking has different effects on heart and skeletal muscle. *J Cachexia Sarcopenia Muscle*. 2018;9:417-432.
23. Souza TA, Chen X, Guo Y, et al. Proteomic identification and functional validation of activins and bone morphogenetic protein 11 as candidate novel muscle mass regulators. *Mol Endocrinol*. 2008;22:2689-2702.
24. Gao E, Lei YH, Shang X, et al. A novel and efficient model of coronary artery ligation and myocardial infarction in the mouse. *Circ Res*. 2010;107:1445-1453.
25. Vainio LE, Szabo Z, Lin R, et al. Connective tissue growth factor inhibition enhances cardiac repair and limits fibrosis after myocardial infarction. *JACC Basic Transl Sci*. 2019;4:83-94.
26. Tolonen AM, Magga J, Szabo Z, et al. Inhibition of Let-7 microRNA attenuates myocardial remodeling and improves cardiac function postinfarction in mice. *Pharmacol Res Perspect*. 2014;2:e00056.
27. Szabo Z, Magga J, Alakoski T, et al. Connective tissue growth factor inhibition attenuates left ventricular remodeling and dysfunction in pressure overload-induced heart failure. *Hypertension*. 2014;63:1235-1240.
28. Vogel B, Siebert H, Hofmann U, Frantz S. Determination of collagen content within picrosirius red stained paraffin-embedded tissue sections using fluorescence microscopy. *MethodsX*. 2015;2:124-134.
29. Ruas JL, White JP, Rao RR, et al. A PGC-1alpha isoform induced by resistance training regulates skeletal muscle hypertrophy. *Cell*. 2012;151:1319-1331.
30. Ueland T, Nymo SH, Latini R, et al. CCL21 is associated with fatal outcomes in chronic heart failure: data from CORONA and GISSI-HF trials. *Eur J Heart Fail*. 2013;15:747-755.
31. Yndestad A, Finsen AV, Ueland T, et al. The homeostatic chemokine CCL21 predicts mortality and may play a pathogenic role in heart failure. *PLoS ONE*. 2012;7:e33038.
32. McPherron AC. Metabolic functions of myostatin and GDF11. *Immunol Endocr Metab Agents Med Chem*. 2010;10:217-231.
33. Zhang C, McFarlane C, Lokireddy S, et al. Inhibition of myostatin protects against diet-induced obesity by enhancing fatty acid oxidation and promoting a brown adipose phenotype in mice. *Diabetologia*. 2012;55:183-193.
34. Sartori R, Schirwis E, Blaauw B, et al. BMP signaling controls muscle mass. *Nat Genet*. 2013;45:1309-1318.
35. Hu J, Wang X, Tang YH, et al. Activin A inhibition attenuates sympathetic neural remodeling following myocardial infarction in rats. *Mol Med Rep*. 2018;17:5074-5080.
36. Morvan F, Rondeau JM, Zou C, et al. Blockade of activin type II receptors with a dual anti-ActRIIA/IIB antibody is critical to promote maximal skeletal muscle hypertrophy. *Proc Natl Acad Sci U S A*. 2017;114:12448-12453.
37. Shi Y, Massague J. Mechanisms of TGF-beta signaling from cell membrane to the nucleus. *Cell*. 2003;113:685-700.
38. Han HQ, Zhou X, Mitch WE, Goldberg AL. Myostatin/activin pathway antagonism: molecular basis and therapeutic potential. *Int J Biochem Cell Biol*. 2013;45:2333-2347.
39. Dschietzig TB. Myostatin - from the mighty mouse to cardiovascular disease and cachexia. *Clin Chim Acta*. 2014;433:216-224.
40. Bezzerides VJ, Platt C, Lerchenmuller C, et al. CITED4 induces physiologic hypertrophy and promotes functional recovery after ischemic injury. *JCI Insight*. 2016;1:1-14.
41. Bostrom P, Mann N, Wu J, et al. C/EBPbeta controls exercise-induced cardiac growth and protects against pathological cardiac remodeling. *Cell*. 2010;143:1072-1083.
42. Zhou X, Wang JL, Lu J, et al. Reversal of cancer cachexia and muscle wasting by ActRIIB antagonism leads to prolonged survival. *Cell*. 2010;142:531-543.
43. Lee SJ, Huynh TV, Lee YS, et al. Role of satellite cells versus myofibers in muscle hypertrophy induced by inhibition of the myostatin/activin signaling pathway. *Proc Natl Acad Sci U S A*. 2012;109:E2353-E2360.
44. Wolfe RR. The underappreciated role of muscle in health and disease. *Am J Clin Nutr*. 2006;84:475-482.
45. Rahimov F, King OD, Warsing LC, et al. Gene expression profiling of skeletal muscles treated with a soluble activin type IIB receptor. *Physiol Genomics*. 2011;43:398-407.

46. Relizani K, Mouisel E, Giannesini B, et al. Blockade of ActRIIB signaling triggers muscle fatigability and metabolic myopathy. *Mol Ther*. 2014;22:1423-1433.
47. Bechir N, Pecchi E, Relizani K, et al. Mitochondrial impairment induced by postnatal ActRIIB blockade does not alter function and energy status in exercising mouse glycolytic muscle in vivo. *Am J Physiol Endocrinol Metab*. 2016;310:E539-E549.
48. Tuomainen T, Tavi P. The role of cardiac energy metabolism in cardiac hypertrophy and failure. *Exp Cell Res*. 2017;360:12-18.
49. Jackson MF, Luong D, Vang DD, et al. The aging myostatin null phenotype: reduced adiposity, cardiac hypertrophy, enhanced cardiac stress response, and sexual dimorphism. *J Endocrinol*. 2012;213:263-275.
50. Biesemann N, Mendler L, Wietelmann A, et al. Myostatin regulates energy homeostasis in the heart and prevents heart failure. *Circ Res*. 2014;115:296-310.
51. Jamaiyar A, Wan W, Janota DM, Enrick MK, Chilian WM, Yin L. The versatility and paradox of GDF 11. *Pharmacol Ther*. 2017;175:28-34.
52. Fang DY, Lu B, Hayward S, de Kretser DM, Cowan PJ, Dwyer KM. The role of activin A and B and the benefit of follistatin treatment in renal ischemia-reperfusion injury in mice. *Transplant Direct*. 2016;2:e87.
53. Palin NK, Savikko J, Pasternack A, et al. Activin inhibition limits early innate immune response in rat kidney allografts-a pilot study. *Transpl Int*. 2017;30:96-107.
54. Egerman MA, Cadena SM, Gilbert JA, et al. GDF11 increases with age and inhibits skeletal muscle regeneration. *Cell Metab*. 2015;22:164-174.
55. Jones JE, Cadena SM, Gong C, et al. Supraphysiologic administration of GDF11 induces cachexia in part by upregulating GDF15. *Cell Rep*. 2018;22:1522-1530.
56. Harper SC, Johnson J, Borghetti G, et al. GDF11 decreases pressure overload-induced hypertrophy, but can cause severe cachexia and premature death. *Circ Res*. 2018;123:1220-1231.
57. Dogra D, Ahuja S, Kim HT, Rasouli SJ, Stainier DYR, Reischauer S. Opposite effects of Activin type 2 receptor ligands on cardiomyocyte proliferation during development and repair. *Nat Commun*. 2017;8:1902.
58. Morissette MR, Stricker JC, Rosenberg MA, et al. Effects of myostatin deletion in aging mice. *Aging Cell*. 2009;8:573-583.
59. Biesemann N, Mendler L, Kostin S, Wietelmann A, Borchardt T, Braun T. Myostatin induces interstitial fibrosis in the heart via TAK1 and p38. *Cell Tissue Res*. 2015;361:779-787.
60. Bo Li Z, Zhang J, Wagner KR. Inhibition of myostatin reverses muscle fibrosis through apoptosis. *J Cell Sci*. 2012;125:3957-3965.
61. Hedger MP, de Kretser DM. The activins and their binding protein, follistatin—diagnostic and therapeutic targets in inflammatory disease and fibrosis. *Cytokine Growth Factor Rev*. 2013;24:285-295.
62. Prabhu SD, Frangogiannis NG. The biological basis for cardiac repair after myocardial infarction: from inflammation to fibrosis. *Circ Res*. 2016;119:91-112.
63. Kleinbongard P, Schulz R, Heusch G. TNFalpha in myocardial ischemia/reperfusion, remodeling and heart failure. *Heart Fail Rev*. 2011;16:49-69.
64. Pistilli EE, Bogdanovich S, Goncalves MD, et al. Targeting the activin type IIB receptor to improve muscle mass and function in the mdx mouse model of Duchenne muscular dystrophy. *Am J Pathol*. 2011;178:1287-1297.
65. Kainulainen H, Papaioannou KG, Silvennoinen M, et al. Myostatin/activin blocking combined with exercise reconditions skeletal muscle expression profile of mdx mice. *Mol Cell Endocrinol*. 2015;399:131-142.
66. Pollari E, Savchenko E, Jaronen M, et al. Granulocyte colony stimulating factor attenuates inflammation in a mouse model of amyotrophic lateral sclerosis. *J Neuroinflammation*. 2011;8:74.
67. Tamargo J, Caballero R, Delpon E. New drugs in preclinical and early stage clinical development in the treatment of heart failure. *Expert Opin Investig Drugs*. 2019;28:51-71.

SUPPORTING INFORMATION

Additional Supporting Information may be found online in the Supporting Information section.

How to cite this article: Szabó Z, Vainio L, Lin R, et al. Systemic blockade of ACVR2B ligands attenuates muscle wasting in ischemic heart failure without compromising cardiac function. *The FASEB Journal*. 2020;00:1–14. https://doi.org/10.1096/fj.201903074RR